NASA
Technical Memorandum 100115
AIAA-87-1745

AVSCOM
Technical Report 87-C-21

Performance of Two 10-lb/sec Centrifugal Compressors With Different Blade and Shroud Thicknesses Operating Over a Range of Reynolds Numbers

Gary J. Skoch
Propulsion Directorate
U.S. Army Aviation Research and Technology Activity—AVSCOM
Lewis Research Center
Cleveland, Ohio

and

Royce D. Moore
Lewis Research Center
Cleveland, Ohio

NASA

N87-23623 Unclas 0077502 G3/07

(NASA-TM-100115) PERFORMANCE OF TWO 10-LB/SEC CENTRIFUGAL COMPRESSORS WITH DIFFERENT BLADE AND SHROUD THICKNESSES OPERATING OVER A RANGE OF REYNOLDS NUMBERS (NASA) 25 p Avail: NTIS HC A02/MF A01

PERFORMANCE OF TWO 10-LB/SEC CENTRIFUGAL COMPRESSORS WITH DIFFERENT

BLADE AND SHROUD THICKNESSES OPERATING OVER A

RANGE OF REYNOLDS NUMBERS

Gary J. Skoch
Propulsion Directorate
U.S. Army Aviation Research and Technology Activity - AVSCOM
Lewis Research Center
Cleveland, Ohio 44135

and

Royce D. Moore
National Aeronautics and Space Administration
Lewis Research Center
Cleveland, Ohio 44135

SUMMARY

A 10-lb/sec, 8:1 pressure ratio, centrifugal compressor was tested at the NASA Lewis Research Center as part of a program to study the effect of scaling centrifugal compressors to small sizes. It was scaled down to 2 lb/sec where adjustments were made to increase the blade thickness and fillet radii. The adjustments were required because of structural and manufacturing considerations. To determine the effect of the modifications, the 2-lb/sec design was directly scaled back up to 10 lb/sec and a second compressor with thicker rotor blades and diffuser vanes was built. Both 10-lb/sec compressors were tested over a range of speed, mass flow, Reynolds number, and tip clearance. Impeller shrouds with two different wall thicknesses were tested to determine the effect on performance of heat transfer from the compressor exit to inlet.

Test results at design speed, with the design tip clearance of 0.009 in., showed that the thin compressor produced a pressure ratio of 7.69, with a total to total adiabatic efficiency of 0.792 at the design mass flow of 10 lb/sec. At the same mass flow and operating condition, the thick compressor produced a pressure ratio of 7.64 with an efficiency of 0.777.

The efficiency loss that occurred as Reynolds number was reduced was found to be dependent on the thickness of the shroud that was used. The exponent commonly used in a relation between loss and Reynolds number was found to be equal to -0.095 for both compressors when tested with the thin shroud, and -0.183 when the thick shroud was used.

The tip clearance of the thin compressor was increased in 0.001 in. increments at design speed with an inlet total pressure of 14 psia. The efficiency was found to decrease about 0.25 points for every 1 percent of blade height increase in tip clearance.

E-3660

INTRODUCTION

Centrifugal compressors provide several performance advantages when used in small gas turbine engines. Among them is the high pressure ratio that can be achieved in a single stage which allows fewer stages to be used in an engine. Centrifugal compressors are also more rugged than small axial compressors and tend to maintain their efficiency better than equivalent axial compressors as flow size is reduced.

Theoretically, for directly scaled compressors of both the axial and centrifugal type, one would expect that the only increase in loss to occur as flow size is reduced would be associated with the lower Reynolds numbers at which the compressor operates; considering standard day inlet conditions as a reference. However, direct scaling to very small sizes is often not possible due to structural considerations and the increased difficulty of manufacture. Because of the inability to directly scale all design parameters, additional losses do result over and above the viscous loss correlated by Reynolds number. It is known that the factors which contribute to additional losses include increased blade and shroud thickness, rougher surfaces in a relative sense, larger fillet radii, etc. But the change in loss caused by individual varia- tions in these parameters is not well known.

The effect of scaling axial compressors to smaller sizes has been well documented, an example of which is given in a study reported by Wiggins and Waltz (ref. 1). A 54-lb/sec, eight-stage axial compressor, was directly scaled (scale factor = 0.304) down to a flow size of 5 lb/sec. The authors were very careful to ensure that all design parameters were directly scaled. Subsequent testing of the scaled compressor showed that the direct scaling of all param eters resulted in no performance loss, other than that which can be attributed to Reynolds number. Other examples of axial compressor scaling can be found in references 2 and 3.

Based on the lack of similar data for centrifugal compressors, and our present inability to calculate centrifugal compressor losses, it was determined that the performance of carefully scaled centrifugal compressors should be investigated. A program was initiated at NASA Lewis to study the effect of scaling centrifugal compressors to small sizes. In flow sizes where all design parameters could not be directly scaled, test data was obtained to quantify the change in efficiency caused by a variation of each parameter. The data obtained from the NASA Lewis program will be useful in developing models that can be used to predict and minimize the performance loss that is caused by the inability to directly scale all parameters.

A 10-lb/sec, 8:1 pressure ratio, centrifugal compressor was tested at NASA Lewis. This compressor was a direct scale (i.e. all dimensions multiplied by $\sqrt{10/25}$) of a 25-lb/sec compressor that was designed and tested by Garrett Turbine Engine Company under a program funded by the Air Force Aeronautical Propulsion Laboratory (AFAPL) at Wright Patterson Air Force Base (ref. 4). The 10-lb/sec compressor and test rig were fabricated for NASA Lewis by Garrett (ref. 5).

The 10-lb/sec compressor was intended to be directly scaled down to a flow size of 2 lb/sec, but practical considerations prevented it. The directly scaled blade thickness and fillet radii would have been less than the minimum

set by current manufacturing capabilities; so the blade thickness and fillet radii were increased from the directly scaled design. The wall thickness of the 2-lb/sec impeller shroud was also increased. A description of the 2-lb/sec aerodynamic design can be found in reference 6. To determine the effect of the nonscaled modifications on performance, the 2-lb/sec design was directly scaled back up to a 10-lb/sec flow size, and a second 10-lb/sec compressor was fabricated (ref. 6) and tested.

The objective of this paper is to present a performance comparison of the two 10-lb/sec compressors. The comparison shows the effect of the modifications to the 2-lb/sec compressor that were scaled up in the design of the second 10-lb/sec compressor. Both compressors were tested over a range of speed, mass flow, Reynolds number and tip clearance. Test results are also presented which show the effect of variations in these parameters on compressor performance.

SYMBOL LIST

b	impeller blade height at exit, in.
CL	impeller axial tip clearance at exit, in.
D	impeller exit tip diameter, ft
N	percent of design equivalent speed
P	total stagnation pressure, psia
p	static pressure, psia
Re	Reynolds number, $\dfrac{\rho_2 U_2 D_2}{\mu_1}$
SM	Surge Margin, $\dfrac{\left(W \cdot \sqrt{\theta}/\delta / P_3/P_1\right)_{ref}}{\left(W \cdot \sqrt{\theta}/\delta / P_3/P_1\right)_{surge}} - 1 \times 100$
T	total stagnation temperature, °R
$T_{surface}$	metal temperature of shroud surface at impeller inlet, °R
ΔT_{shroud}	temperature difference between shroud surface at inlet and inlet gas temperature, $(T_{surface} - T_1)$, °R
ΔT_{stage}	temperature rise associated with compressor work input, $(T_3 - T_1)$, °R
U	impeller tip speed, ft/sec
W	compressor mass flow, lbm/sec

δ	ratio of compressor inlet total pressure to U.S. standard sea level pressure, $P_1/14.7$ psia
η	adiabatic temperature rise efficiency, $\dfrac{\text{ideal total enthalpy rise}}{\text{actual total enthalpy rise}}$
θ	ratio of compressor inlet total temperature to U.S. standard sea level temperature, $T_1/518.7$
μ	viscosity, lbm/ft·sec
ρ	stagnation density at inlet, lbm/ft^3
Ω	mass flow speed parameter, $[(W/N)/(W/N)_{design}]$
ω	diffuser loss coefficient, $(P_3 - P_2)/(P_2 - p_2)$

Subscripts

1	station in inlet plenum tank, figure 4
2	station at compressor exit, figure 4
3	station at downstream of diffuser exit, figure 4

COMPRESSOR AERODYNAMIC DESIGN

The 10-lb/sec compressor with thin blades (ref. 5) is a direct scale (scale factor = $\sqrt{10/25}$) of the 25-lb/sec AFAPL compressor. This scale factor was applied to the cold coordinates of impeller, diffuser, and shroud contours of the 25-lb/sec compressor. It was also applied to the design tip clearance of the 25-lb/sec stage which resulted in a tip clearance of 0.009 in. in the 10-lb/sec compressor. The aerodynamic design of the 25-lb/sec AFAPL compressor is given in reference 4.

The 10-lb/sec compressor with thick blades is a direct scale (scale factor = $\sqrt{10/2}$) of the modified 2-lb/sec compressor. The thick 10-lb/sec impeller and diffuser are shown in figure 1. The modifications that were made to the 2-lb/sec stage mainly involved increases in blade thickness and fillet radii in the impeller and diffuser. A direct scale of the thin 10-lb/sec compressor down to a 2-lb/sec flow size required a minimum blade thickness of 0.007 in. It was determined that the minimum practical thickness for the impeller and diffuser blades was 0.012 in., so 0.005 in. was added to all normal thickness values. The impeller throat area and exit blade height of the 2-lb/sec compressor were adjusted to provide the same choke margin and work input as the thin 10-lb/sec compressor. A complete description of the design procedure that was used to adjust the 2-lb/sec compressor is given in reference 6.

Cross sections of the thick and thin shrouds are shown in figure 2. The thin compressor was tested with both shrouds, the thick compressor was tested with the thin shroud only. Both shrouds had surface temperature thermocouples located near the impeller inlet.

4

The mechanical designs of the thin and thick compressors can be found in references 5 and 6, respectively. A summary of the design geometry and estimated performance of each compressor is given below.

	Thin	Thick
Impeller		
Number of main blades/splitters	20/20	20/20
Inlet tip radius, in.	4.172	4.172
Inlet hub radius, in.	2.052	2.052
Exit radius, in.	6.319	6.319
Exit tip width, in.	0.403	0.417
Design exit tip clearance, in.	0.009	0.009
Diffuser		
Number of full vanes/splitter vanes	21/21	21/21
Vane inlet radius, in.	6.775	6.775
Splitter inlet radius, in.	7.124	7.124
Vane exit radius, in.	8.349	8.349
Diffuser passage height, in.	0.386	0.395
Vane L.E. thickness, in.	0.013	0.027
Vane T.E. thickness, in.	0.063	0.089
Splitter L.E. thickness, in.	0.013	0.027
Splitter T.E. thickness, in.	0.054	0.089
Total Throat Area (sq. in.)	5.904	5.898
Stage		
Corrected mass flow, lbm/sec	10	10
Stage total pressure ratio, P_3/P_1	7.8	<7.8
Stage total temperature ratio, T_3/T_1	1.950	1.950
Stage total efficiency, η_{1-3}	0.827	<0.827
Corrected speed, rpm	36 366	36 366
Corrected exit tip speed, ft/sec	2 007	2 007

APPARATUS AND PROCEDURE

Compressor Test Facility

The centrifugal compressor test facility was designed for a maximum flow rate of 13 lb/sec, a maximum pressure of 300 psia, and a maximum discharge temperature of 800 °F. A schematic of the facility is shown in figure 3. Atmospheric air enters from a filter house located on the roof of the building. A vaned elbow straightens the flow ahead of the orifice run, which is 16 diameters of straight pipe upstream of the removable orifice plate and 5 diameters downstream. Two inlet valves control the compressor inlet pressure at a predetermined value, ranging from 2 psia to atmospheric (minus line losses). The 16-in. butterfly valve is manually controlled for coarse adjustments and the 6-in. butterfly valve is automatically controlled for fine adjustment.

Another vaned elbow is used downstream of the inlet throttle valve to straighten the flow into a 36-in. plenum tank. A 5.5 wires/in. screen is located in the plenum to condition the flow before it enters a bellmouth which provides a transition from the plenum to the compressor inlet.

The compressed air flows into a collector where the flow is controlled by a throttle valve. The throttle valve rotates in a circumferential direction to expose portions of three 2-in. diameter holes located at the collector discharge. The air is discharged back to atmosphere through a pipe which exits through the test cell roof.

The compressor is driven by an electric motor through a two-stage gear box with an overall gear ratio of 11.330:1. The induction motor develops 3000 hp at 3588 rpm. Motor speed is determined by a magnetic speed pickup from a 38 tooth gear.

Instrumentation

Compressor mass flow is determined from the upstream orifice located in the air inlet pipe. The orifice flow is calculated using the standard ASME orifice flow equations for 1 D - 1/2 D pressure taps. Orifice temperature is determined from an average of two chromel-constantan thermocouples located just upstream of the orifice plate. Orifice pressure and delta pressure are each determined from averages of two calibrated pressure transducer readings.

Compressor speed is directly measured by a magnetic speed pickup located over a six tooth sleeve that rotates with the compressor shaft. This measurement is compared with the motor and gear box shaft speeds which are multiplied by the appropriate gear ratio to determine compressor speed. A thermocouple reading taken in the plenum tank is used to calculate the corrected speed.

Compressor measurement stations are shown in figure 4. Inlet conditions were measured in the plenum tank (measurement station 1). Inlet total temperature was measured with two bare wire chromel-constantan thermocouples. Inlet total pressure was obtained from an average of two calibrated pressure transducers connected to pressure taps in the plenum tank. Eight static pressure taps were spaced evenly around the impeller exit tip (measurement station 2).

The compressor exit measurement station 3 was located just downstream of the bend in the exit discharge passage. Total temperature measurements were obtained from eight total temperature rakes which were calibrated for Mach number effects and spaced around the exit passage circumference. Each total temperature rake contained three chromel-alumel elements located at 10, 50, and 90 percent of exit passage height. Exit total pressure measurements at station 4 were obtained from six four-element rakes, located at 8, 34, 60, and 86 percent of exit passage height. The exit passage hub and shroud each contained four equally spaced wall statics that were at the same axial location as the total pressure and temperature rakes.

All research pressure readings downstream of the plenum were measured with scanning type valves that use a single calibrated pressure transducer which is accurate to ±0.1 percent of full scale. Thermocouples are connected to a floating point reference. Measured temperatures are accurate to ±1 °R. The data has been corrected to standard day conditions based on the plenum tank measurements.

Tip Clearance Measurement

The test rig was equipped with a clearance control mechanism (fig. 4) which allowed the impeller to be translated forward or aft during operation. The impeller to shroud axial clearance was measured using graphite rub probes. A description of the clearance control mechanism is given in reference 5.

A deflection versus rotational speed curve was determined for each impeller at the start of the test program. A baseline measurement of rub probe length was established with the impeller set at an extreme aft position and rotating at less than 1000 rpm. The change in rub probe length was then measured after operation at 60, 70, 80, 90, and 100 percent of design speed. The probes were measured after operating a mid-flow point for approximately one-half hour and again after a compressor surge at each speed. At 100 percent speed the measurements indicated that the impeller exit tip deflected an additional 0.009 in. during surge.

Test Procedure

Stage performance data were taken at speeds of 60, 70, 80, 90, and 100 percent of design speed. Operating clearance was set by adding the design speed mid-flow deflection to the required tip clearance (0.009 in.) and moving the impeller to the proper starting point. The graphite rub probes were measured after each test to verify that the impeller had actually been at the desired axial tip clearance. At speeds below design, the clearance was greater than 0.009 in. because there was less impeller deflection.

At each speed the mass flow was varied from choke to near surge using the compressor exit throttle. Compressor surge was determined by an increase in compressor noise which was accompanied by instability in analog (x-y recorder) measurements of compressor mass flow and pressure ratio. Because the additional deflection of the impeller at surge was equal to the operating clearance of 0.009 in., the surge point was found only once at design speed with an initial clearance set point of 0.018 in.

At each speed the Reynolds number was set by changing the inlet total pressure, which varied the inlet stagnation density. The inlet total pressure and speed were held constant as mass flow was reduced. At design speed the compressor was tested at five Reynolds numbers corresponding to inlet total pressures of 3, 6, 9, 12, and 14 psia. The inlet pressure could not be reduced as far as speeds below 100 percent because the compressor pressure rise at low speed was not high enough to overcome exhaust system losses. At 60 and 70 percent speed, 9 psia was the lowest inlet pressure that could be used. At 80 and 90 percent it was 6 psia.

A test of efficiency change with clearance was conducted on the thin compressor, thin shroud configuration. The peak efficiency point was found for design speed at the design tip clearance of 0.009 in. The clearance control mechanism was then used to increase the tip clearance by 0.001 in. and the throttle was adjusted until peak efficiency was found at the new clearance. The procedure was repeated until the impeller to shroud axial clearance was 0.027 in.

Performance Calculation Procedure

The pressure and temperature ratios were determined from arithmetic aver-ages of the total pressures and temperatures at station 3 and measurements in the plenum tank. A polynomial curve fit of gas table properties for air, which accounts for the change in specific heat over a large temperature rise, was used to find the enthalpy rise. Efficiency was determined by comparing the ideal and actual total enthalpy rise.

The measured total temperature at station 3, the measured static pressure at the impeller exit (station 2), and the orifice mass flow measurement were used to calculate the total pressure at the impeller exit. The calculation procedure was based on continuity and the Euler work equations. The flow area was calculated from the impeller exit tip diameter and the blade height plus clearance at the impeller exit. No aerodynamic blockage was assumed. Impeller efficiency was determined the same was as stage efficiency, except that the total pressure used was the calculated total pressure at the impeller exit.

The diffuser loss coefficient (ω) is based on the calculated impeller exit total pressure, the measured static pressure at station 2, and the measured total pressure at station 3.

RESULTS AND DISCUSSION

Stage Performance

The overall performance of each compressor operating with an inlet pressure of 14 psia is presented in figure 5. Total pressure ratio, tempera-ture rise, and adiabatic efficiency based on total conditions are presented as a function of equivalent mass flow for five speeds. The tip clearance was 0.009 inches at design speed. At the design equivalent tip speed of 2007 ft/sec and the design equivalent mass flow of 10 lb/sec, the thin com-pressor produced a pressure ratio of 7.69 with a total adiabatic efficiency of 0.792. At the same equivalent speed and mass flow, the thick compressor produced a pressure ratio of 7.64 with a total efficiency of 0.777. The results presented above are from tests using the thin shroud.

The design speed peak efficiency of both compressors occurred at the design mass flow of 10 lb/sec. The thick compressor provided more energy addition at that flow but did not achieve a corresponding increase in pressure. In figure 5, the temperature rise of the thin compressor at the design mass flow was 0.98, compared to 1.00 for the thick compressor. The higher work input of the thick compressor at design flow is probably due to the slight increase in exit blade height that was incorporated in the 2-lb/sec design. This increase was scaled up to 10 lb/sec along with all other modifications that were made in the 2-lb/sec design. The lack of a corresponding increase in pressure indicates that the thick compressor had higher losses due to the increased blade thickness and fillet radii in the impeller and diffuser.

The thin compressor demonstrated higher performance at all speeds. The efficiency increased with speed from 0.753 at 60 percent to a maximum of 0.798 at 90 percent speed. At design speed the efficiency of thin compressor decreased slightly to 0.792. This fall off is explained in the next section.

8

The efficiency of the thick compressor steadily rises with speed from 0.750 at 60 percent to 0.777 at 100 percent except for a 0.006 drop at 70 percent. The reasons for this drop are not known.

Based on the pressure ratio obtained at the design mass flow of 10 lb/sec, the thin compressor had a design speed surge margin (SM) of 10.5 percent compared to 7.7 percent for the thick compressor. The difference in surge margin is primarily due to a difference in the pressure ratio of each compressor at surge. For the thin compressor, the pressure ratio continued to rise as the mass flow was reduced. The pressure ratio and temperature rise of the thick compressor flattened out at 98 percent of design flow and remained fairly constant as the mass flow was further reduced. This pattern suggests that the flow through the thick impeller became more highly separated as flow was reduced.

Both compressors had a choke flow rate of 10.2 lb/sec at design speed. A mass flow-speed parameter (Ω) (described by Klassen, Wood, and Schumann, ref. 7) is plotted as a function of speed for the thin and thick compressors in figure 6. A positive slope between two points indicates diffuser controlled flow, a negative slope indicates inducer controlled flow. In figure 6 the slope of each line segment is positive, indicating a diffuser controlled flow up to design speed for both the thick and thin compressors.

Component Performance

The individual component performances of the thin and thick compressors are presented in figure 7 for the same operating conditions as the stage data that were presented in figure 5. Impeller total pressure, impeller adiabatic efficiency based on total conditions, and diffuser loss coefficient are shown as a function of mass flow for five speeds.

The peak efficiency of the thin impeller increased with speed from 3.876 at 60 percent speed to 0.901 at design speed. The impeller showed almost no increase in efficiency between 90 and 100 percent speed, but the diffuser loss coefficient went from 0.284 to 0.301. The slight (0.006) decrease that was observed in overall stage efficiency at design speed in figure 5 is thus attributed to the increase in the loss coefficient of the thin diffuser at design speed.

The efficiency of the thick impeller was lower over the speed range and only reached 0.890 at design speed. The minimum loss in the thick diffuser was also higher at all speeds. The data presented in figure 7 show that the non-scaled modifications included in the design of the thick compressor lowered the performance of both the impeller and diffuser.

Effect of Reynolds Number on Performance

The stage performance of both compressors over a range of Reynolds number is shown in figure 8. Stage total pressure ratio, total temperature rise, and adiabatic efficiency are presented as a function of design equivalent mass flow for five Reynolds numbers. The data shown were obtained at design speed with 0.009 in. of exit tip clearance. The operating point of interest in obtaining

this data was the peak efficiency point of each speed line, therefore the surge point was not obtained at every Reynolds number.

As the Reynolds number was reduced the maximum pressure ratio, peak efficiency, and equivalent mass flow where peak efficiency occurred, decreased in both compressors. The same trends were reported in earlier work by Heidelberg, Ball, and Weigel (ref. 8) on a 6-in centrifugal compressor. The explanation given in reference 8 can also be applied to the results presented here.

The reduced equivalent mass flow at peak efficiency is explained in terms of an increase in boundary layer thickness that occurs as the Reynolds number is reduced. The increased boundary layer thickness causes a reduction in the effective flow area in the impeller, which increases the impeller through flow velocity at a given mass flow. If the relative flow angle leaving the impeller is assumed to remain constant, the higher through flow velocity will cause a reduction in the absolute flow angle leaving the impeller and entering the diffuser. As the flow rate is reduced by closing the compressor exit throttle, the through flow velocity is reduced to the point where the optimum flow angle is once again achieved. However, since the effective impeller flow area has not been changed by closing the throttle, the equivalent mass flow where the optimum flow angle again occurs must be lower.

The increase in through flow velocity should also result in a reduction in compressor work input at the lower Reynolds numbers. As figure 8 shows, the total temperature rise, and therefore the work input of both compressors did decrease with Reynolds number. The reduction in total temperature rise was greater for the thick compressor over nearly the same range of Reynolds number.

The decrease in pressure ratio of the thick compressor was also greater over the same Reynolds number range. However the peak efficiency change in both compressors was about the same over this range; -0.031 and -0.038 for the thin and thick compressors, respectively. The difference is within experimental accuracy, which leads one to conclude that the additional loss in pressure ratio of the thick compressor can probably be attributed to the corresponding loss in work input.

In general, the pressure loss that is caused by a reduction in Reynolds number cannot be attributed to a reduction in work input only. The peak efficiency points from each Reynolds number in figure 8 are cross plotted in figure 9 which shows efficiency loss (1 - eff) as a function of Reynolds number.

A common relation between efficiency loss (1 - eff) and Reynolds number is

$$\frac{(1 - eff)}{(1 - eff)_{ref}} = \left[\frac{Re}{(Re)_{ref}}\right]^{n}$$

where $(1 - eff)_{ref}$ and $(Re)_{ref}$ are known values of loss and Reynolds number. The exponent represents the rate of efficiency loss with Reynolds number for individual compressors.

Straight lines have been fitted to the data in figure 9. The data are plotted on logarithmic scales so that the slope of each line corresponds to a value of the exponent in the equation above. The values obtained for each line are in good agreement between the two compressors. They are -0.0939 and 0.0947 for the thick and thin compressors, respectively. The thick compressor had higher efficiency loss at all Reynolds numbers, which again shows the effect of the increased blade thickness and fillet radii.

Effect of Shroud Thickness on Efficiency

The stage performance of the thin compressor as influenced by Reynolds number and shroud thickness is shown in figure 10. The dashed line shows the variation in loss with Reynolds number for the thin compressor when tested with the thin (thermally scaled) shroud. It is the same data presented on the dashed line in figure 9. The solid line is the variation of loss with Reynolds number for the thin compressor when tested with the thick (containment) shroud. The efficiency loss is approximately the same for both configurations at Reynolds numbers approaching the design Reynolds number of 1.33×10^7. As the Reynolds number is reduced the configuration with the thick shroud losses efficiency much more rapidly than the one with the thin shroud. The value of the exponent for the thick shroud configuration is -0.1834, compared to a value of -0.0947 for the thin shroud. Reasons for this shroud thickness effect are discussed next.

The results of temperature measurements from shroud surface thermocouples (see fig. 2) that were located at the impeller inlet on the outside surface of each shroud are shown in figure 11. The parameter along the ordinate of figure 11 is the difference between the average shroud surface temperature and the bulk fluid temperature entering the compressor inlet (ΔT_{shroud}) which has been nondimensionalized by the overall compressor temperature rise (ΔT_{stage}). The overall compressor temperature rise represents the maximum potential driving mechanism for heat transfer. This parameter is presented as a function of Reynolds number for the thin and thick shrouds.

If the same heat transfer coefficient exists between the inner surface of either shroud and the fluid stream at a given Reynolds number, then figure 11 shows the potential for heat transfer from the shroud to the air stream by virtue of the temperature difference. The temperature difference, and therefore the heat transfer, increased as the Reynolds number was reduced with both shrouds. However, the increase in heat transfer with decreasing Reynolds number is much greater for the thick shroud.

Heat transfer from the shroud to the fluid stream will result in lower compressor efficiency. The effect is interheating which works in the opposite direction of stage intercooling and lowers efficiency. The trend of efficiency loss with Reynolds number in figure 10 is very similar to the trend of shroud heat transfer with Reynolds number in figure 11. At high Reynolds numbers the difference in loss between the two shrouds approaches zero. The heat transfer parameters for each shroud also approach the same value as the Reynolds number increases. The similarity in the trends, displayed by the efficiency loss in figure 10 and the heat transfer to the compressor inlet in figure 11, suggests that stage interheating was the cause of the higher loss when the Reynolds number was reduced with the thick shroud.

Effect of Tip Clearance on Performance

The variation of peak stage efficiency with tip clearance at design speed with ambient inlet pressure is shown in figure 12. The data shown are a combination of the data obtained from 0.001-in. variations in tip clearance, and the peak efficiency points from speed line tests. A linear decrease of about 0.25 points (0.0025) in efficiency for every 1 percent of blade height increase in tip clearance is shown.

SUMMARY OF RESULTS

The performance of two 10-lb/sec centrifugal compressors was investigated. The compressors had different blade thickness and fillet radii and were tested over a range of speed, mass flow, Reynolds number, and tip clearance. The effect of shroud thickness on compressor performance was also investigated. The major results of this investigation are as follows:

1. At the design speed of 2007 ft/sec and the design mass flow of 10 lb/sec the thin compressor produced a pressure ratio of 7.69 with an adiabatic efficiency of 0.792. At the same operating conditions the thick compressor produced a pressure ratio of 7.64 with an adiabatic efficiency of 0.777.

2. Performance calculations for the individual components showed that the lower performance of the thick compressor was due to both lower impeller efficiency and higher diffuser pressure loss.

3. The change in efficiency with Reynolds number was nearly the same for both compressors when tested with the same shroud. The exponent used in the loss versus Reynolds number relation was -0.0939 for the thin compressor and -0.0947 for the thick compressor.

4. Measurements of the shroud surface temperature at the compressor inlet indicated that the reason for the higher loss from the thick shroud was the recirculation of heat to compressor inlet. The heat transfer to the compressor inlet caused a stage interheating effect which lowered performance.

5. The efficiency of the thin compressor decreased about 0.25 points for every 1 percent of blade height increase in tip clearance.

REFERENCES

1. Wiggins, J.O. and Waltz, G.L., "Some Experiences in the Scaling of the NASA 8-Stage Transonic Axial Flow Compressor," SAE Paper 720711, Sept. 1972.

2. Sawyer, C.W. III, "Evaluation of a Low Aspect Ratio Small Axial Compressor Stage," PWA-FR-8499-VOL-1, Pratt a Whitney Aircraft Group, West Palm Beach, FL, Nov. 1977. (NASA CR-135240).

3. Holman, F.F., Kidwell, J.R., and Ware, T.C., "Small Axial Compressor Technology Program," AIRESEARCH-74-310862-VOL-1, -VOL-2, AiResearch Manufacturing Co., Phoenix, AZ, June 1976. (NASA CR-134827-VOL-1, -VOL-2).

4. Clarke, R.C., Waterman, W.F., and Palmreuter, F., "Turbine Engine Centrifugal Compressor Technology Program," AIRESEARCH-21-0820(52), AiResearch Manufacturing Co., Phoenix, AZ, Aug. 1978. (Also, AFAPL-TR-78-66, Avail. NTIS as AD-C016469L).

5. Kenehan, J.G., "Scaled Centrifugal Compressor, Collector and Running Gear Program," GR-21-4269, Garrett Turbine Engine Co., Phoenix, AZ, Oct. 1983. (NASA CR-168167).

6. Cargill, G. and Linder, C., "Scaled Centrifugal Compressor Program," GARRETT-21-5464, Garrett Turbine Engine Co., Phoenix, AZ, Oct. 1986. (NASA CR-174912).

7. Klassen, H.A., Wood, J.R., and Schumann, L.F., "Experimental Performance of a 16.10-Centimeter-Tip-Diameter Sweptback Centrifugal Compressor Designed for a 6:1 Pressure Ratio," NASA TM X-3552, 1977.

8. Heidelberg, L.J., Ball, C.L., and Weigel, C., "Effect of Reynolds Number On Overall Performance of a 6-Inch Radial Bladed Centrifugal Compressor," NASA TN D-5761, 1970.
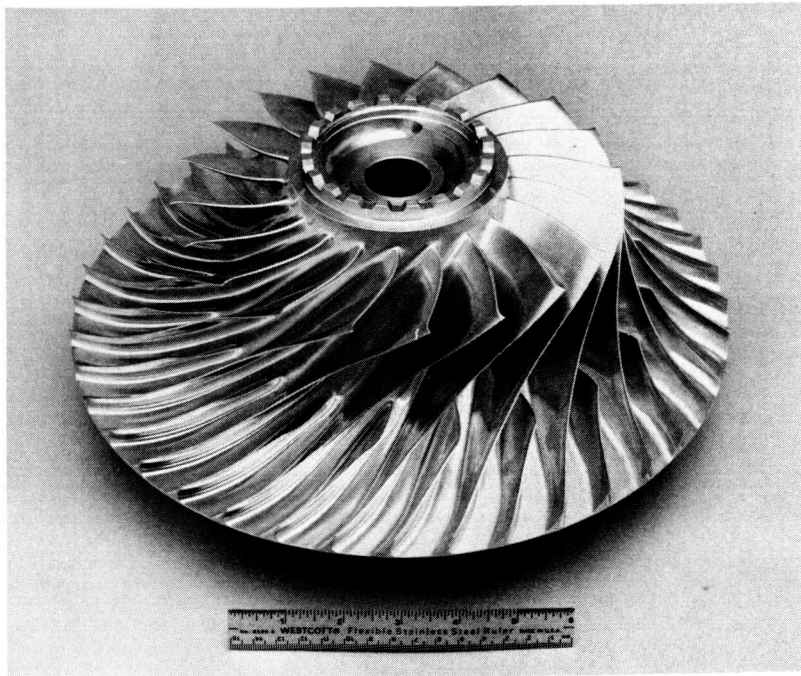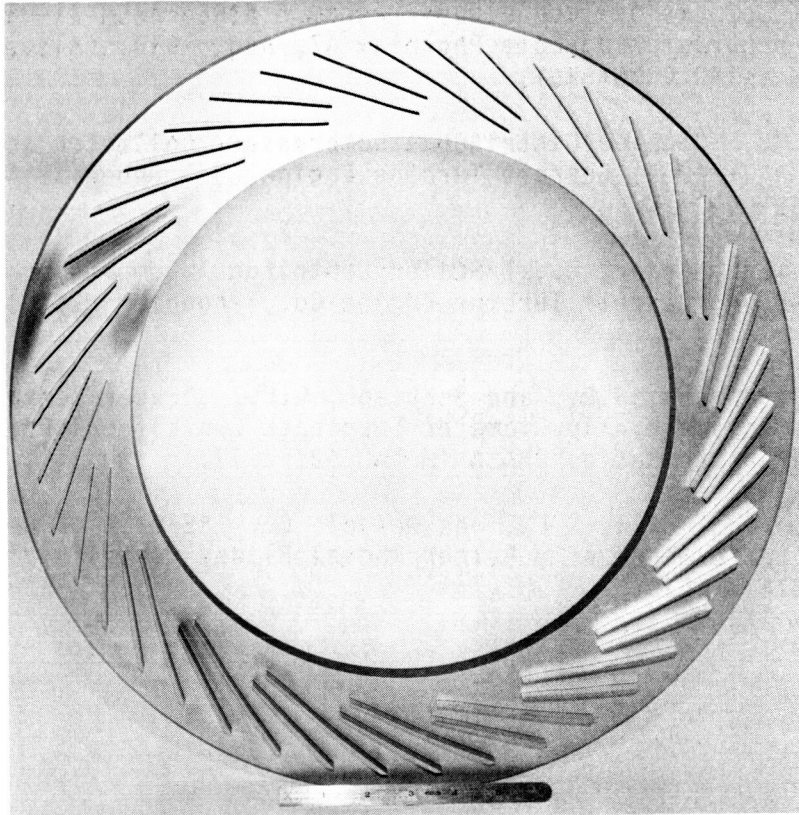
FIGURE 1. - IMPELLER AND DIFFUSER FROM 10 LB/SEC THICK BLADED
CENTRIFUGAL COMPRESSOR.

SHROUD SURFACE
THERMOCOUPLES

THIN SHROUD

0.158 IN.

IMPELLER

SHROUD SURFACE
THERMOCOUPLES

THICK SHROUD

1.225 IN.

IMPELLER
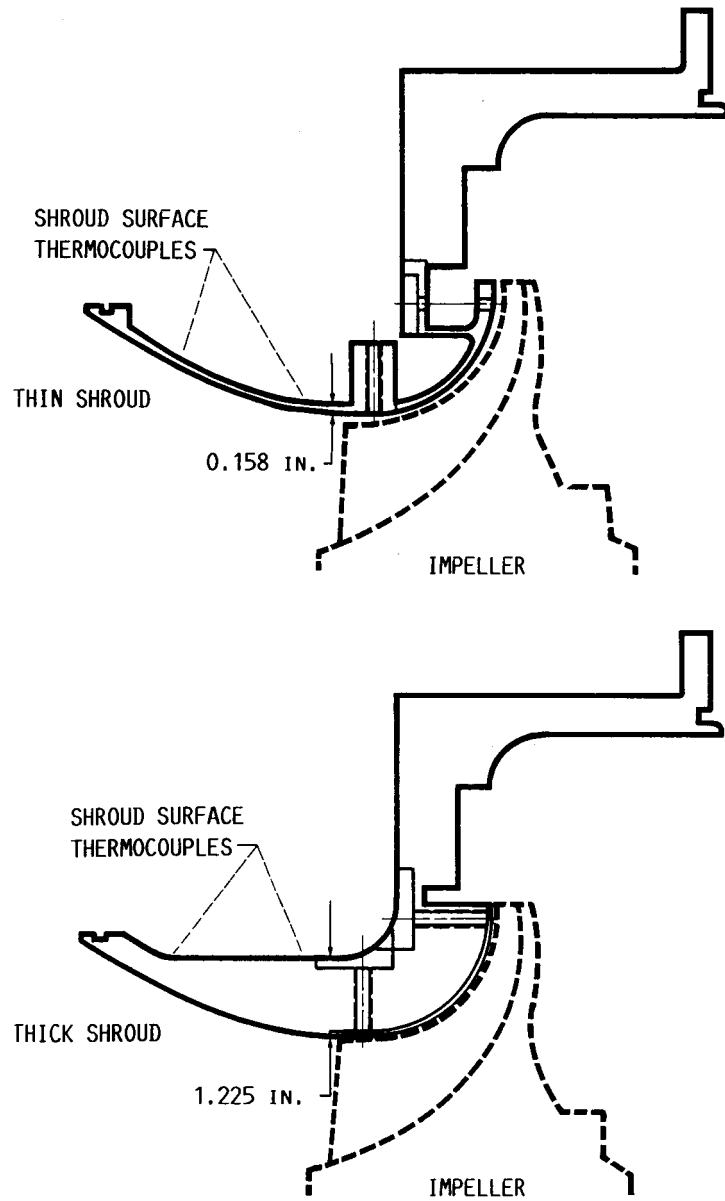
FIGURE 2. - CROSS SECTIONS OF THICK AND THIN COMPRESSOR SHROUDS.

FACILITY CAPABILITIES

MAXIMUM AIRFLOW, LB/SEC 13
MAXIMUM ROTATIVE SPEED, RPM 60 000
PLENUM PRESSURE, PSIA . . . . 2 TO 14
DISCHARGE PRESSURE, PSIA 300
MAXIMUM OUTLET TEMPERATURE, ^{0}F 800
ACTIVE CLEARANCE CONTROL. . . . .

ATMOSPHERE EXHAUST

ORIFICE

ATMOSPHERE AIR

16 IN. BUTTERFLY VALUE

VANED ELBOW

3000 HP VARIABLE SPEED DRIVE MOTOR

COLLECTOR THROTTLE VALUE

6 IN. BUTTERFLY VALVE

VANED ELBOW

STRAIGHTENED SCREEN

RESEARCH COMPRESSOR

PLENUM CHAMBER

TWO-STAGE SPEED INCREASING GEARBOX

COLLECTOR
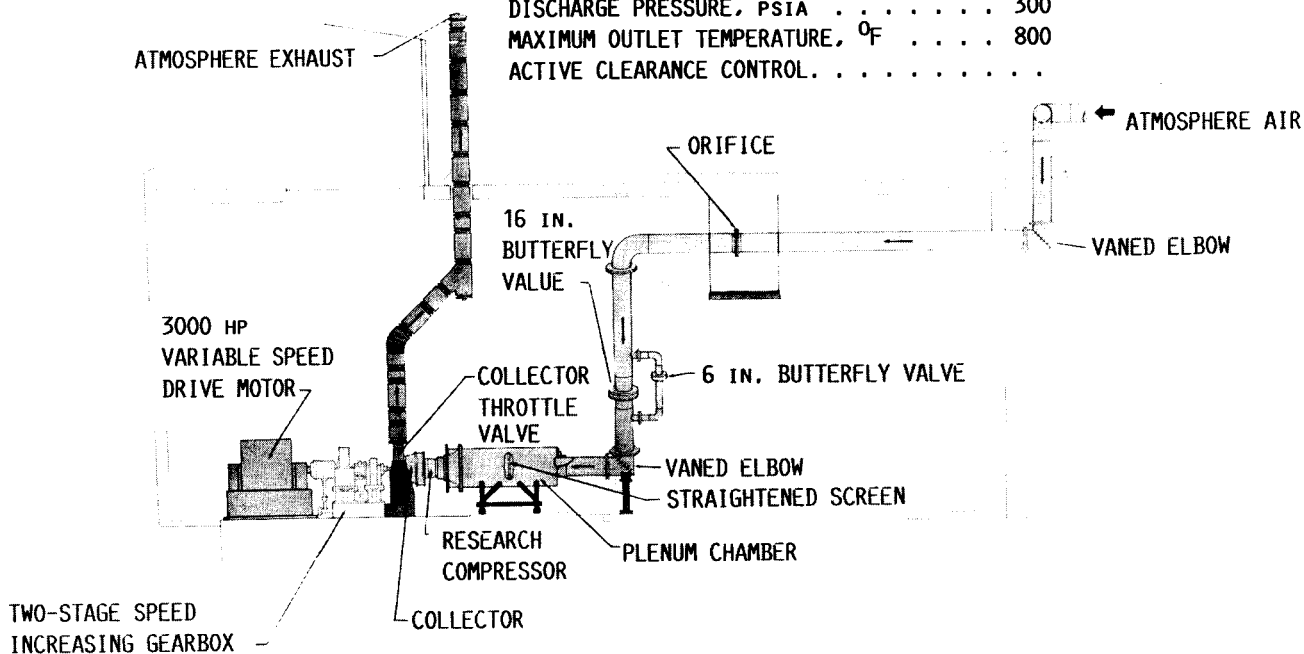
FIGURE 3. - CENTRIFUGAL COMPRESSOR TEST FACILITY.

16
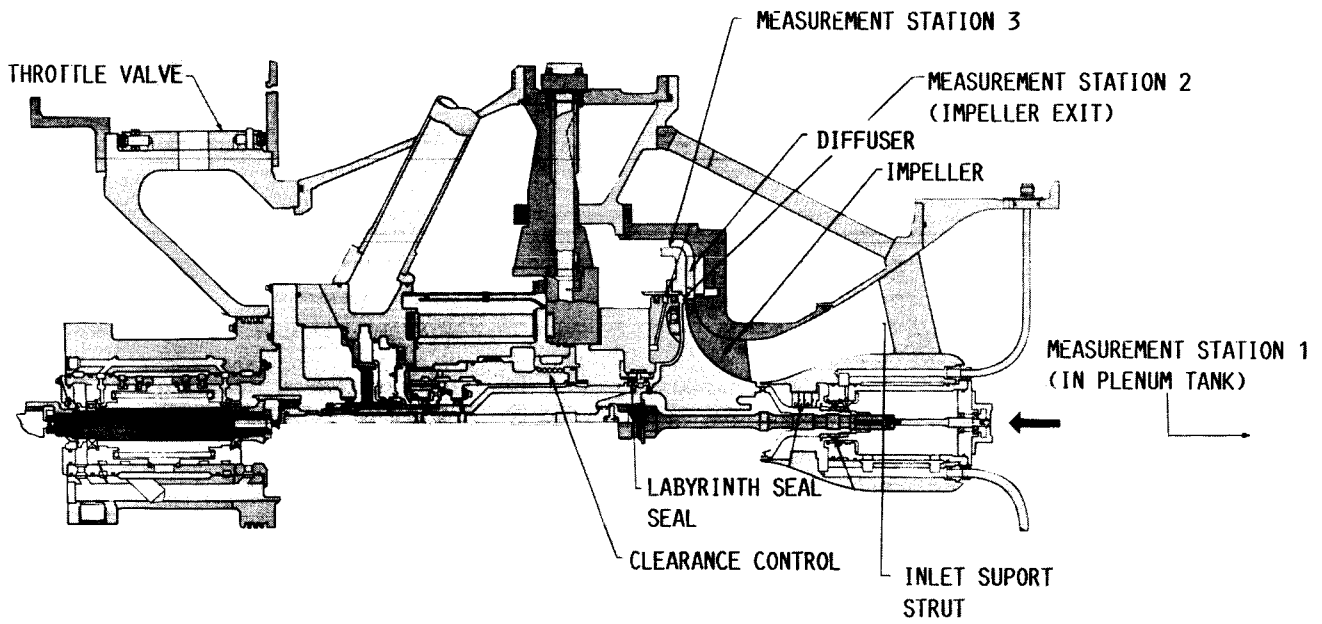
FIGURE 4. - CENTRIFUGAL COMPRESSOR TEST RIG.
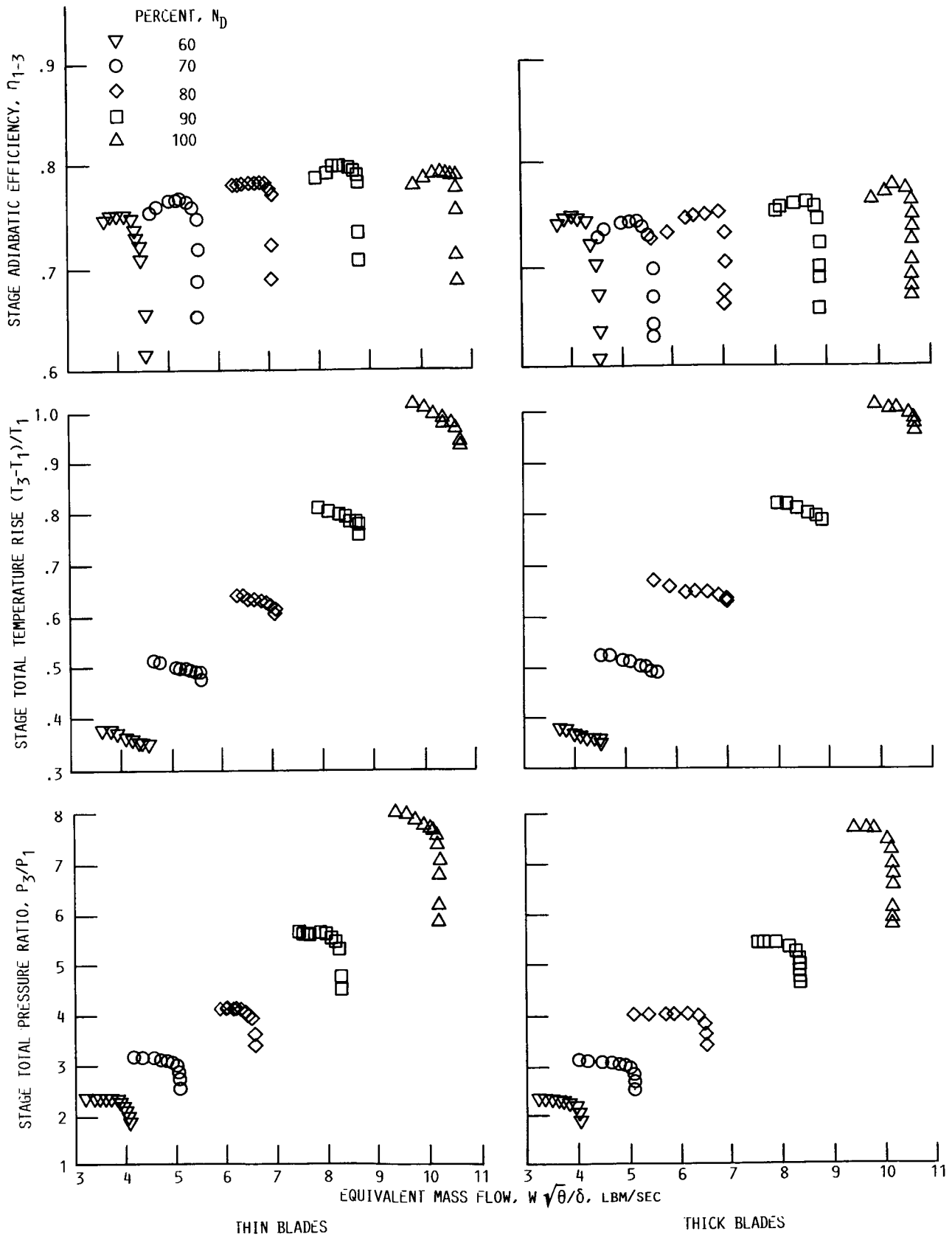
FIGURE 5. - OVERALL PERFORMANCE OF TWO 10 LB/SEC COMPRESSORS WITH THIN AND THICK BLADES OPERATING OVER A RANGE OF SPEED WITH A THIN SHROUD AND ATMOSPHERIC INLET PRESSURE.
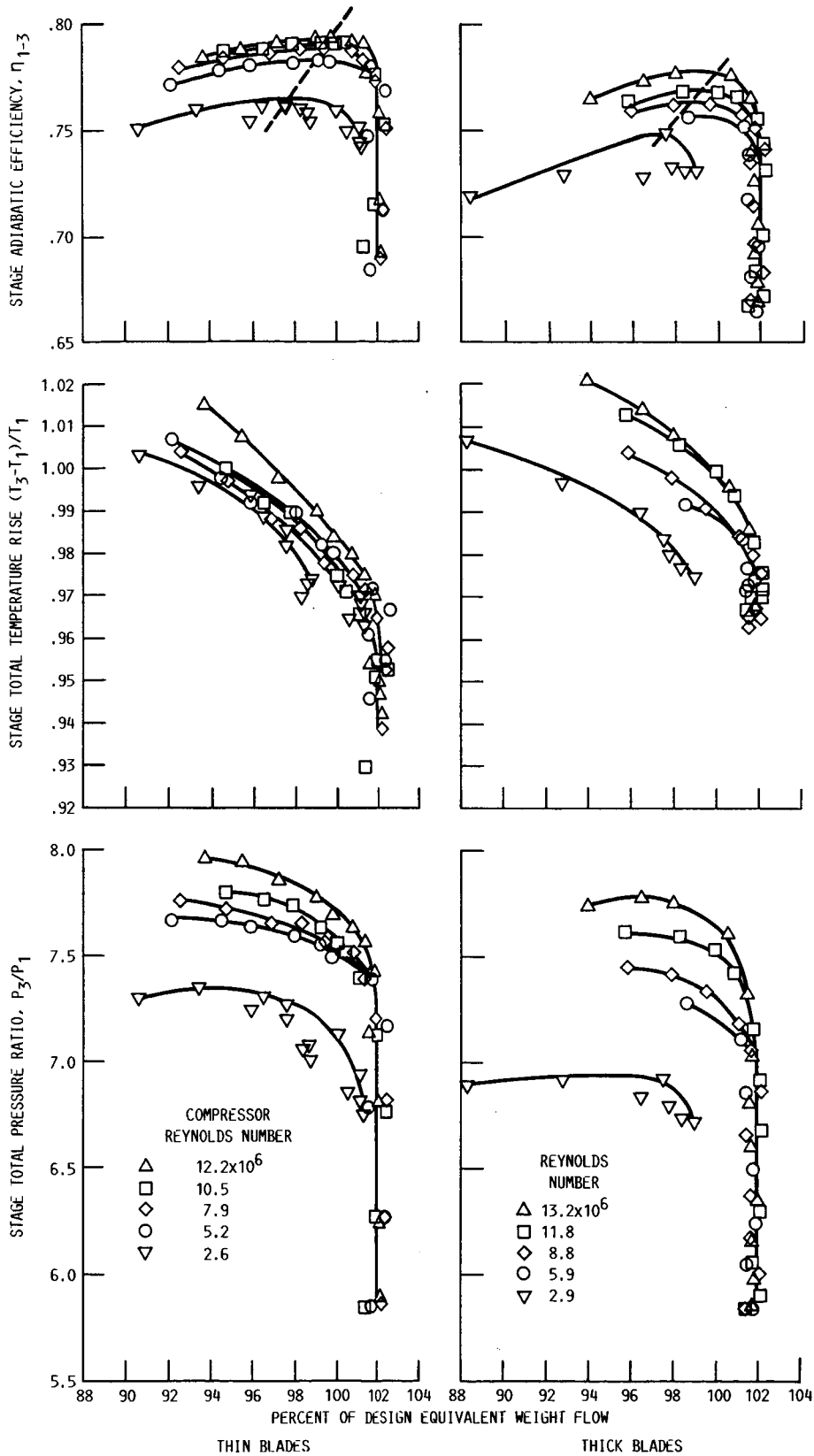
18
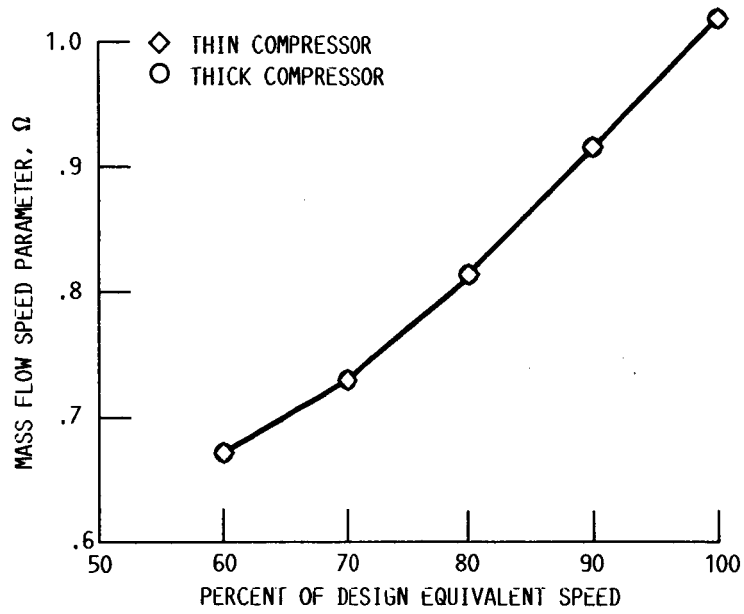
FIGURE 6. - MASS FLOW-SPEED PARAMETER FOR CHOKE FLOW
OVER A RANGE OF SPEED FOR THIN AND THICK COMPRESSORS
OPERATING WITH ATMOSPHERIC INLET PRESSURE.
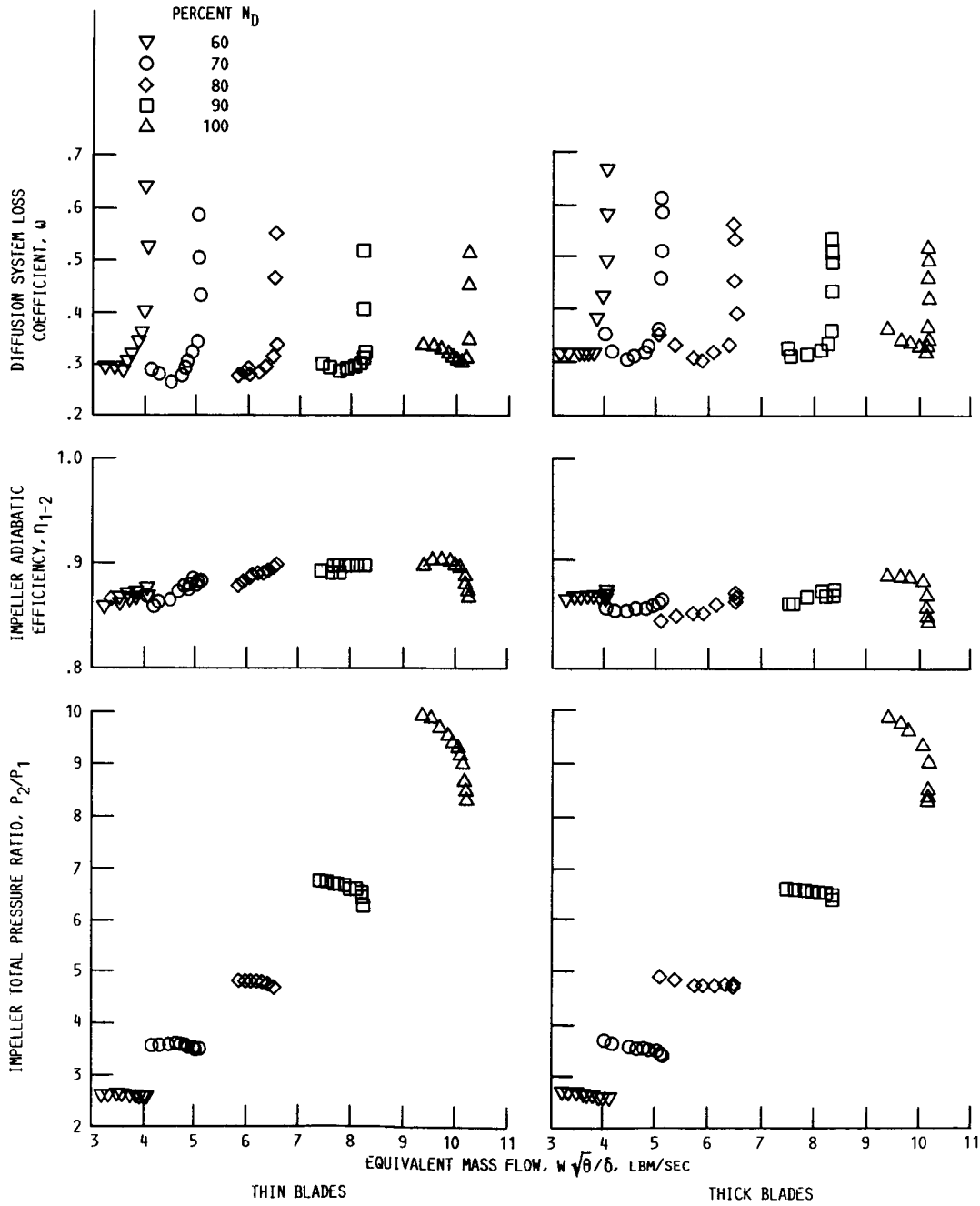
FIGURE 7. - COMPONENT PERFORMANCE OF TWO 10 LB/SEC COMPRESSORS WITH THIN AND THICK BLADES OPERATING OVER A RANGE OF SPEED WITH A THIN SHROUD AND ATMOSPHERIC INLET PRESSURE.

20

FIGURE 8. - COMPARISON OF COMPRESSOR PERFORMANCE OVER A RANGE OF REYNOLDS NUMBERS AT
DESIGN SPEED AND TIP CLEARANCE.
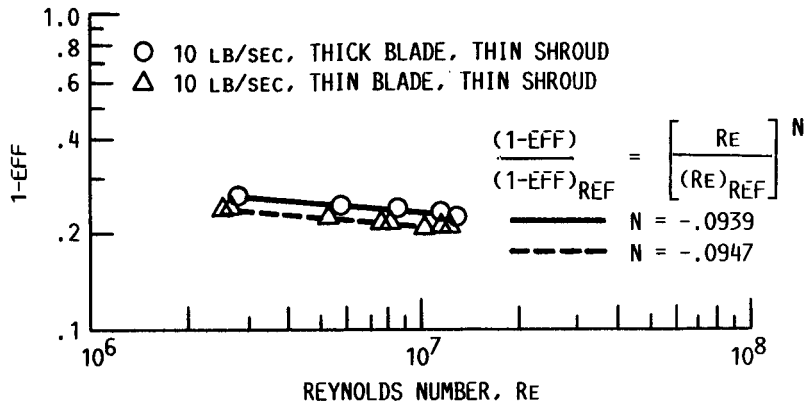
FIGURE 9. - EFFICIENCY LOSS WITH REYNOLDS NUMBER FOR
TWO 10 LB/SEC COMPRESSORS WITH THIN AND THICK BLADES
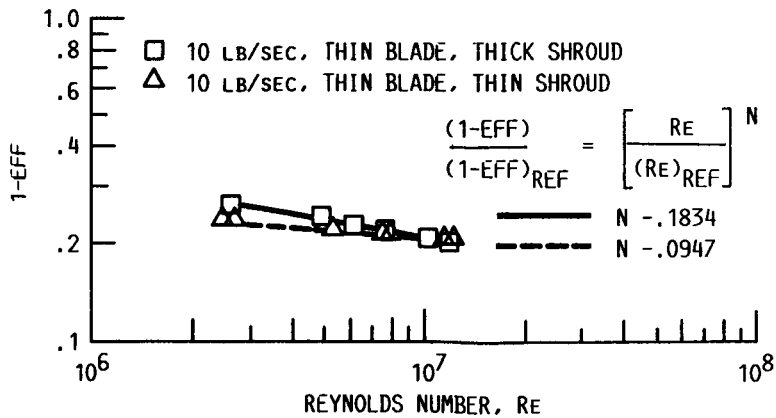TESTED WITH A THIN SHROUD AT 100 PERCENT OF DESIGN
SPEED.

FIGURE 10. - EFFICIENCY LOSS WITH REYNOLDS NUMBER FOR
A 10 LB/SEC COMPRESSOR WITH THIN BLADES TESTED WITH A
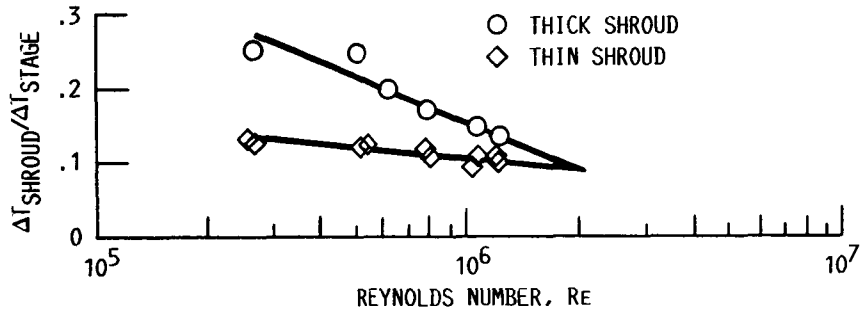THICK AND THIN SHROUD AT 100 PERCENT OF DESIGN SPEED.

FIGURE 11. - VARIATION OF TEMPERATURE DIFFERENCE BETWEEN
SHROUD SURFACE AND INLET BULK FLUID TEMPERATURE AS A PER-
CENT OF STAGE TOTAL TEMPERATURE RISE FOR 10 LB/SEC COMPRESSOR
WITH THIN BLADES OPERATING AT 100 PERCENT OF DESIGN SPEED
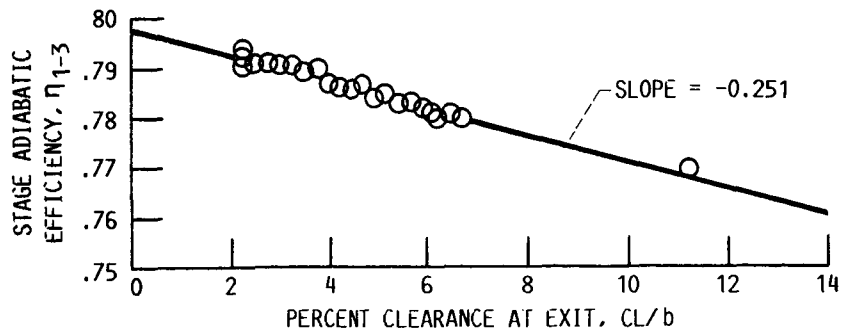OVER A RANGE OF REYNOLDS NUMBERS.

FIGURE 12. - VARIATION IN PEAK STAGE EFFICIENCY WITH EXIT
TIP CLEARANCE FOR 10 LB/SEC COMPRESSOR WITH THIN BLADES
OPERATING AT 100 PERCENT OF DESIGN SPEED.

23

NASA

National Aeronautics and
Space Administration

Report Documentation Page

1. Report No. NASA TM-100115 AIAA-87-1745; AVSCOM TR-87-C-21	2. Government Accession No.	3. Recipient's Catalog No.
4. Title and Subtitle Performance of Two 10-lb/sec Centrifugal Compressors With Different Blade and Shroud Thicknesses Operating Over a Range of Reynolds Numbers		5. Report Date
		6. Performing Organization Code 535-05-01
7. Author(s) Gary J. Skoch and Royce D. Moore		8. Performing Organization Report No. E-3660
		10. Work Unit No.
9. Performing Organization Name and Address NASA Lewis Research Center and Propulsion Directorate, U.S. Army Aviation Research and Technology Activity – AVSCOM, Cleveland, Ohio 44135		11. Contract or Grant No.
12. Sponsoring Agency Name and Address National Aeronautics and Space Administration Washington, D.C. 20546 and U.S. Army Aviation Systems Command, St. Louis, Mo. 63120		13. Type of Report and Period Covered Technical Memorandum
		14. Sponsoring Agency Code

15. Supplementary Notes

16. Abstract

Centrifugal compressors often can not be directly scaled to very small flow sizes because of structural and manufacturing limitations. The inability to directly scale all design parameters leads to a performance loss other than that which can be associated with the lower Reynolds Number. A 10-lb/sec centrifugal compressor was scaled down to 2 lb/sec where adjustments to blade and shroud thickness and fillet radii were required. The modified 2-lb/sec compressor was then directly scaled back up to 10 lb/sec so that the effect of the modifications could be determined. The performance of the two 10-lb/sec compressors is compared over a range of speed and mass flow. The effect of variations in Reynolds Number, impeller tip clearance, and shroud thickness on compressor performance is also presented.

17. Key Words (Suggested by Author(s)) Turbomachinery; Centrifugal Compressor; Scale; Reynolds number; Blade Thickness	18. Distribution Statement Unclassified – unlimited STAR Category 07

19. Security Classif. (of this report) Unclassified	20. Security Classif. (of this page) Unclassified	21. No of pages 24	22. Price* A02